A common mechanism underlies stretch activation and receptor activation of TRPC6 channels

Maria A. Spassova*, Thamara Hewavitharana, Wen Xu, Jonathan Soboloff, and Donald L. Gill*

Department of Biochemistry and Molecular Biology, University of Maryland School of Medicine, Baltimore, MD 21201

Edited by Solomon H. Snyder, The Johns Hopkins University School of Medicine, Baltimore, MD, and approved September 15, 2006 (received for review August 11, 2006)

The TRP family of ion channels transduce an extensive range of chemical and physical signals. TRPC6 is a receptor-activated nonselective cation channel expressed widely in vascular smooth muscle and other cell types. We report here that TRPC6 is also a sensor of mechanically and osmotically induced membrane stretch. Pressure-induced activation of TRPC6 was independent of phospholipase C. The stretch responses were blocked by the tarantula peptide, GsMTx-4, known to specifically inhibit mechanosensitive channels by modifying the external lipid-channel boundary. The GsMTx-4 peptide also blocked the activation of TRPC6 channels by either receptor-induced PLC activation or by direct application of diacylglycerol. The effects of the peptide on both stretch- and diacylglycerol-mediated TRPC6 activation indicate that the mechanical and chemical lipid sensing by the channel has a common molecular mechanism that may involve lateral-lipid tension. The mechanosensing properties of TRPC6 channels highly expressed in smooth muscle cells are likely to play a key role in regulating myogenic tone in vascular tissue.

GsMTx-4 peptide | mechanosensitivity | tarantula venom | myogenic tone | calcium signals

The superfamily of TRP cation channels transduce a remarkable spectrum of signals ranging from small second-messenger molecules to physical parameters including temperature, osmolarity, and touch (1, 2). Among the several subfamilies of TRP channels, the TRPC nonselective cation channels activated in response to PLC-coupled receptors are widely expressed among tissues (2, 3). The closely related subgroup comprising TRPC3, TRPC6, and TRPC7 channels are directly activated by diacylglycerol through a PKC-independent mechanism (3, 4). TRPC6 channels are highly expressed in a number of different tissues including vascular smooth muscle cells (5–8). Despite their abundance, the exact physiological role of TRPC6 channels has not been elucidated. Recently it has been suggested that TRPC6 channels are involved in hemodynamic regulation (6, 9) and may play a role in generating myogenic tone in response to intravascular pressure in arteries (6, 9). This is a key mechanism to control blood flow in arteries and arterioles (10, 11) involving depolarization, activation of Ca^{2+} entry, and the contraction of vascular smooth muscle cells (11). Increases in Ca^{2+} in response to pressure not only activate smooth muscle cell contraction but also modify their growth and differentiation (12). However, the identity and gating mechanisms of the mechanical sensors that mediate the depolarizing response have not been identified.

TRPC6 channels are expressed predominantly in cells responding to hydrostatic pressure changes including vascular smooth muscle and glomerular podocytes and have been implicated in mediating pressure-induced responses (6, 13). TRPC6 channels mediate receptor-induced depolarization in smooth muscle cells (7, 9), and opening of the related TRPC1 channel has been shown to be activated by stretch (14). In addition to being implicated in generating myogenic tone in arteries (6, 9), elevated expression of TRPC6 channels has been linked to smooth muscle proliferation in patients with idiopathic pulmonary arterial hypertension (15). TRPC6 is also shown to be essential for proper function of podocytes that are exposed to hydrostatic pressure driving glomerular ultrafiltration in the kidney (13).

In view of the connections between TRPC6 channels and pressure regulation, we investigated the role of mechanical stretch on TRPC6 channels function. We report here that the TRPC6 channel functions as a direct sensor of mechanically and osmotically induced membrane stretch. These stretch responses are blocked by the tarantula peptide, GsMTx-4, a specific peptide inhibitor of mechanosensitive channels which disturbs the lipid-channel boundary (16, 17). The TRPC6 channel is also activated by receptor-induced PLC activation, an effect mediated by diacylglycerol (DAG) through a PKC-independent mechanism (18, 19). The GsMTx-4 peptide blocked both receptor- and DAG-induced TRPC6 activation. The effects of the peptide on both stretch- and DAG-mediated TRPC6 activation indicate that both chemical lipid sensing as well as mechanical lipid sensing by the channel have a common molecular basis. Moreover, because TRPC6 channels are highly expressed in vascular smooth muscle cells, the results indicate that TRPC6 channel activation by stretch may play a crucial role in mediating control of myogenic tone.

Results and Discussion

In our studies to assess a link between TRPC6 channels and pressure regulation, we investigated the role of mechanical stretch on TRPC6 channels function. Indeed, it was recently revealed that TRPC1 channels are modified by stretch (14). We initially assessed whether TRPC6 channels have a direct involvement in pressure-sensing using a HEK293 cell line inducibly expressing TRPC6 channels (20). Application of a hypoosmotic external medium induced an outwardly rectifying current in cells in which TRPC6 expression was induced by 10 μM ponasterone for 48 h (Fig. 1 *A* and *B*). In control HEK293-TRPC6 cells, in which TRPC6 expression was not induced, there was only a very small hypoosmotic response (<10%; Fig. 1 *C* and *D*), indicating that TRPC6 mediates the current in Fig. 1 *A* and *B*. An increase in capacitance in control cells was observed under the hypoosmotic conditions, increasing ≈7% in 400 sec (Fig. 1*C Inset*) and average of 3 ± 1% during the first 100 sec ($n = 3$). The exclusion of Cl^- ions (replaced by glutamate in these experiments) prevents the contribution of volume-regulating anion channels widely expressed in cells. Similar stretch activation was achieved in CHO cells expressing TRPC6 channels (data not shown). All

Author contributions: M.A.S. and D.L.G. designed research; M.A.S., T.H., and J.S. performed research; W.X. contributed new reagents/analytic tools; M.A.S. analyzed data; and M.A.S. and D.L.G. wrote the paper.

The authors declare no conflict of interest.

This article is a PNAS direct submission.

Abbreviation: DAG, diacylglycerol.

*To whom correspondence may be addressed at: Department of Biochemistry and Molecular Biology, University of Maryland School of Medicine, 108 North Greene Street, Baltimore, MD 21201. E-mail: mspas001@umaryland.edu or dgill@umaryland.edu.

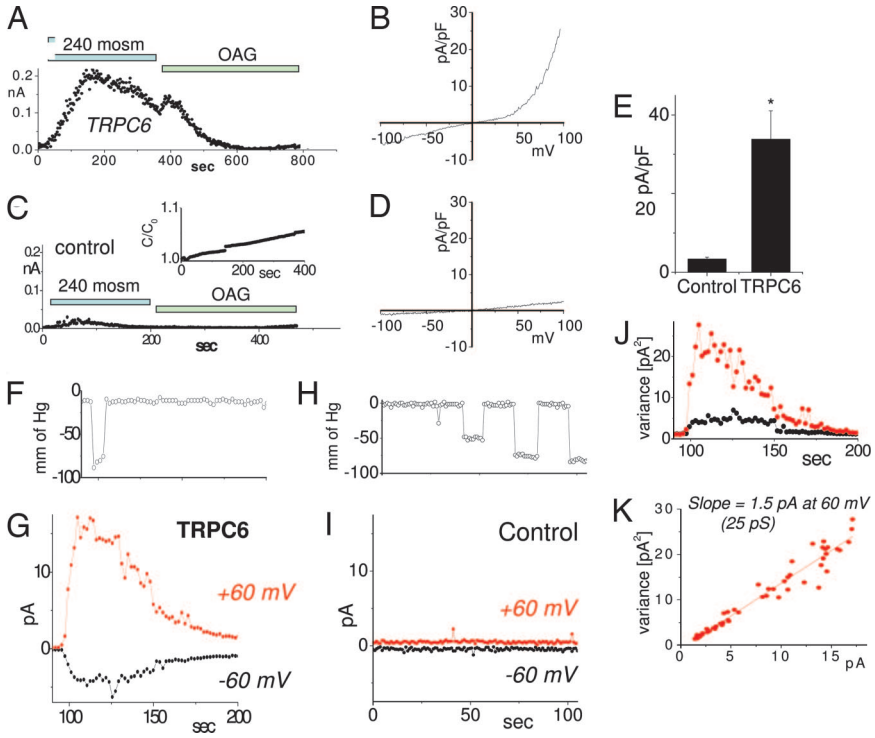

Fig. 1. Hypoosmotic- and pressure-induced stretch activation of nonselective cation current through TRPC6 channels. Currents were measured in HEK293 cells inducibly expressing TRPC6 or in isolated patches from CHO cells transiently expressing TRPC6. (*A*) In HEK293 cells induced to express TRPC6, a current of ≈200 pA at 80 mV developed after exposure to hypoosmotic extracellular solution. Cl^- was substituted with glutamate to prevent volume-regulating Cl^- currents. Addition of the TRPC6 agonist OAG did not induce further current. (*B*) The I/V relationship at maximal activation reveals typical TRPC6-like outward rectification. (*C*) In uninduced HEK293 cells, hypoosmotic- or OAG-induced currents were drastically reduced. Capacitance change during hypoosmotic swelling showed linear time dependence (*Inset*), and the I/V curve (*D*) revealed much reduced amplitude and slight outward rectification. (*E*) Summary of maximal currents at +100 mV for control ($n = 3$) and TRPC6-expressing cells ($n = 4$). (*F–K*) CHO cells, transiently expressing TRPC6, were used to study responses to directly applied pressure pulses. Time course of negative pressure applied to inside-out membrane patches from CHO-TRPC6 cells (*F*). Time course of activation of outwardly rectifying current after pressure pulse (*G*). Each point represents average current recorded for 150 ms at 60 mV (red) and −60 mV (black). Time courses of negative pressure and currents at ±60 mV in control transfected cells are shown in *H* and *I*, respectively. (*J*) Time course of the variance of the current in *G*. (*K*). Variance-current dependence revealed a single-channel conductance of activated channels of 25 pS, typical for TRPC6.

recordings were undertaken with Cs-glutamate based extracellular and intracellular solutions to measure only nonselective cation channels. TRPC6 is a nonselective cation channel with reversal potential close to zero under normal conditions. We detected a negative reversal potential of −10 mV (Fig. 1 *B* and *D*; see also Fig. 3*B*) that reflects the cation concentration gradient under low osmolarity conditions. A statistical summary of the currents at 100 mV for TRPC6-expressing and control cells is presented on Fig. 1*E*. OAG, a membrane permeable DAG derivative, is a known TRPC6 channel agonist (18). We used OAG to investigate whether hypoosmolarity and OAG competed for the same channel target. Addition of OAG after hypoosmotic activation of TRPC6 activated only a minimal current (Fig. 1*A*) compared with the addition of OAG alone (see Fig. 3*J*) indicating that the hypoosmolarity-activated current is likely through the TRPC6 channel.

To assess whether the activation of TRPC6 was directly in response to membrane stretch, we used isolated membrane patches from CHO cells overexpressing TRPC6. CHO cells were used because they have a lower background of stretch-activated cation channels (14). By using isolated membrane patches, membrane stretch was induced by negative pressure applied to the patch pipette. Application of a 5-sec pressure pulse of ≈75 mm of Hg activated an outwardly rectifying current observed only in CHO cells overexpressing TRPC6 (Fig. 1 *F* and *G*) and not in the control CHO cells transfected with the YFP marker (Fig. 1 *H* and *I*). Repeated application of pressure pulses of increasing size revealed that the channel was activated when the pressure reached a threshold of 84 ± 15 mm of Hg (see Fig. 3*E*). We determined single-channel conductance from noise analysis. The stretch-activated current showed a single-channel conductance of 25 pS at +60 mV (Fig. 1 *J* and *K*), in good agreement with the TRPC6 single-channel conductance under similar ionic conditions (21). The noise analysis did not show saturation of the current amplitude, suggesting low open probability of the channels.

An important question was whether the activation of TRPC6 channels by stretch was a downstream effect of stretch-activated receptors coupled to activation of phospholipase C (PLC) (18). Stretch activation of TRPC6 channels in isolated inside-out CHO cell patches was still observed in the presence of the PLC inhibitor U73122 (Fig. 2). As shown in Fig. 2 *A–D*, we examined the single-channel properties after a short pressure pulse (≈2-sec duration), inducing a slower onset of current. We were able to observe single channel events of ≈25 pS even during the pressure pulse application (Fig. 2*C*; 0 sec) confirming the TRPC6 identity of the activated channels. The current before the stimulus showed no channel activity (Fig. 2*C*; −7 sec). A further 7 sec after the pulse, multiple channel openings of similar conductance were observed with higher open probability at positive potentials (Fig. 2*C*; 7 sec.). The continuous activation of current may reflect residual tension in the patch resulting from membrane adhesion to the inside surface of the pipette that occurred during pressure application (22). The difference in the rate of channel response to shorter and longer pressure pulses may reflect potentiation by locally elevated Ca^{2+} entering through TRPC6 channels which are known to be poten-

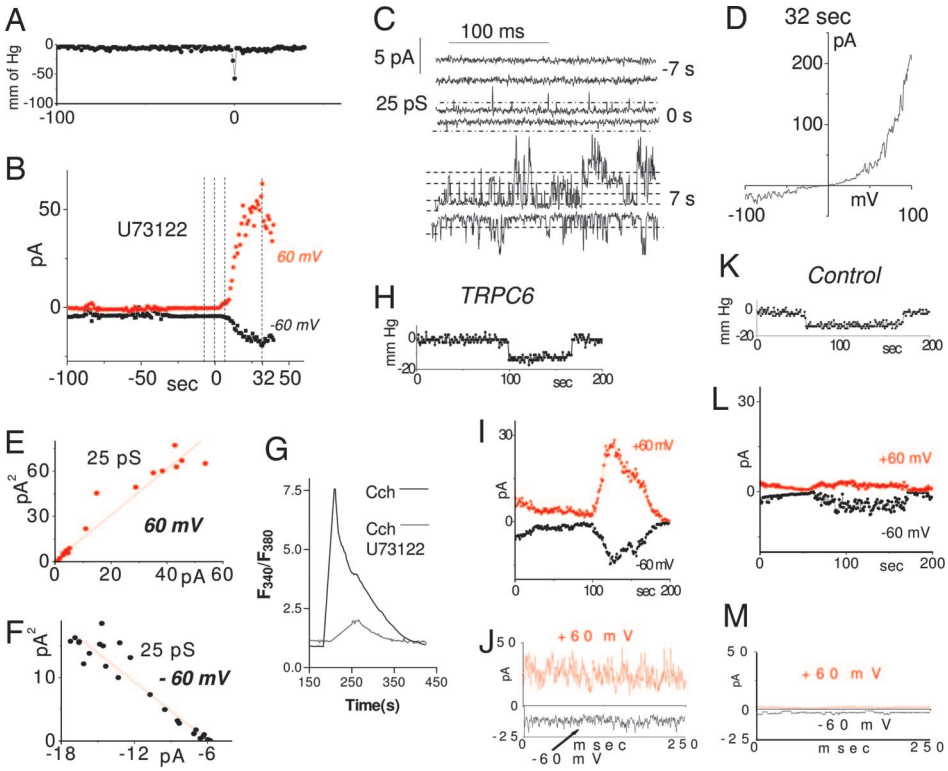

Fig. 2. Time course and phospholipase C-independence of stretch-induced TRPC6 channel activation in CHO cells. (*A–F*) The PLC inhibitor U73122 was used to block possible activation of TRPC6 by PLC-linked stretch-activated receptors. TRPC6 was activated by a short (≈2 sec) pressure pulse (*A*) applied to inside-out membrane patches after >2 min of exposure to 10 μM U73122. (*B*) Average current at −60 mV (black) and +60 mV (red). (*C*) Actual current traces at −60 and +60 mV corresponding to indicated time points in *B*, that is, either 7 s prior (−7s), during (0 s), or 7 s after (+7 s) the pressure pulse. (*D*) Current–voltage dependence of the maximally activated current in *B* recorded by applying a 50-ms voltage ramp from −100 to +100 mV. (*E* and *F*) Noise analysis of the currents from B at +60 and −60 mV, respectively, revealing single-channel conductance of 25 pS. (*G*) Ca^{2+} release in response 100 μM carbachol in HEK cells in the absence of extracellular Ca^{2+} measured by Fura-2 in the presence (red) and absence (black) of 10 μM U73122. (*H–M*) Stretch activation of TRPC6 channels after 40-min incubation of CHO cells in 40 μM cytochalasin D. (*H–J*) Stretch-activated current from inside-out patch of TRPC6 expressing CHO cells. The current has typical TRPC6 outward rectification and short open times. (*H*) Time course of pressure applied to the patch. (*I*) Parallel time course of channel activation. (*J*) High time-resolution current at maximal activation in *I*. (*K–M*) Stretch activation in control cells, showing activation of distinct inwardly rectifying channels with long open times. Usually only 1 or 2 channels were present. (*K*) Time course of pressure applied to inside-out patch. (*L*) Parallel time course of current activation in control cells. (*M*) High time-resolution current from *L*.

tiated by Ca^{2+} (21). As shown in Fig. 2*D*, the macrocurrent generated after a further 25 sec shows the typical TRPC6 outwardly rectifying I/V curve. Noise analysis of the currents showed the same single-channel conductance as observed in Fig. 1*J* (25 pS) at either +60 mV (Fig. 2*E*) or −60 mV (Fig. 2*F*) under our symmetrical 145 mM Cs^{+} conditions. These experiments provide evidence that TRPC6 channels become rapidly activated by stretch through a PLC-independent mechanism. We verified the effectiveness of PLC-blockade by U73122 by examining receptor-induced Ca^{2+} release in HEK cells, which revealed ≈90% reduction (Fig. 2*G*)

Two major classes of stretch activated channels exist: those requiring the fibrous proteins of the cytoskeleton to transmit force to the channel and those responding to stress mediated through the lipid bilayer (16, 23). We investigated a cytoskeletal role in the stretch-gated response of TRPC6 channels by examining stretch activation in the cell-attached mode after prior (40 min) incubation in 40 μM cytochalasin D (Fig. 2 *H–M*). Cytochalasin D treatment enhanced both the time-dependence and the pressure-threshold of the stretch activation of TRPC6 channels. Thus, under this condition, the time course of stretch activation of TRPC6 much more closely followed the time course of the stretch stimulus (Fig. 2 *H–J*). These data suggest that the delayed activation of TRPC6 observed in the absence of cytochalasin D is because of cytoskeletal constraints on membrane dynamics. Moreover, elimination of the actin cytoskeleton with cytochalasin D lowered the pressure threshold of TRPC6 channels activated in CHO cells (Fig. 2 *H–J*; see also Fig. 3*E*). The enhancing effect of cytoskeletal breakdown on stretch-activation of TRPC6 channels provides further evidence that the effect is mediated by lipid bilayer stress alone (23). In addition to this effect on TRPC6 channels, prior cytochalasin D treatment also caused background stretch-activated currents to increase (Fig. 2 *K–M*). However, these currents were inwardly rectifying with single-channel conductance of 40 pS and long open times of >10 msec (Fig. 2 *K–M*), clearly distinct from TRPC6 channels.

TRPC6 channels, like other TRPC channels, contain a number of ankyrin-like repeat sequences (2), perhaps signifying association with the cytoskeleton. A naturally occurring mutation P112Q in one of the TRPC6 ankyrin repeats has been linked to a familial focal segmental glomerulosclerosis (24, 25). The studies demonstrated that TRPC6 is expressed in the glomerular podocytes, which control hydrostatic pressure-driven ultrafiltration. TRPC6 channel functioning in the slit diaphragm plays an essential role in regulation of podocyte structure and function (13), and it was suggested that TRPC6 might be responding to mechanical force (25). We examined the P112Q mutant and found that the current–voltage relationship was preserved, and the stretch sensitivity of the TRPC6-P112Q mutant appeared similar to the wild type (see summary in Fig. 3*E*). Hence, it is unlikely that this mutation is involved in altered responses to

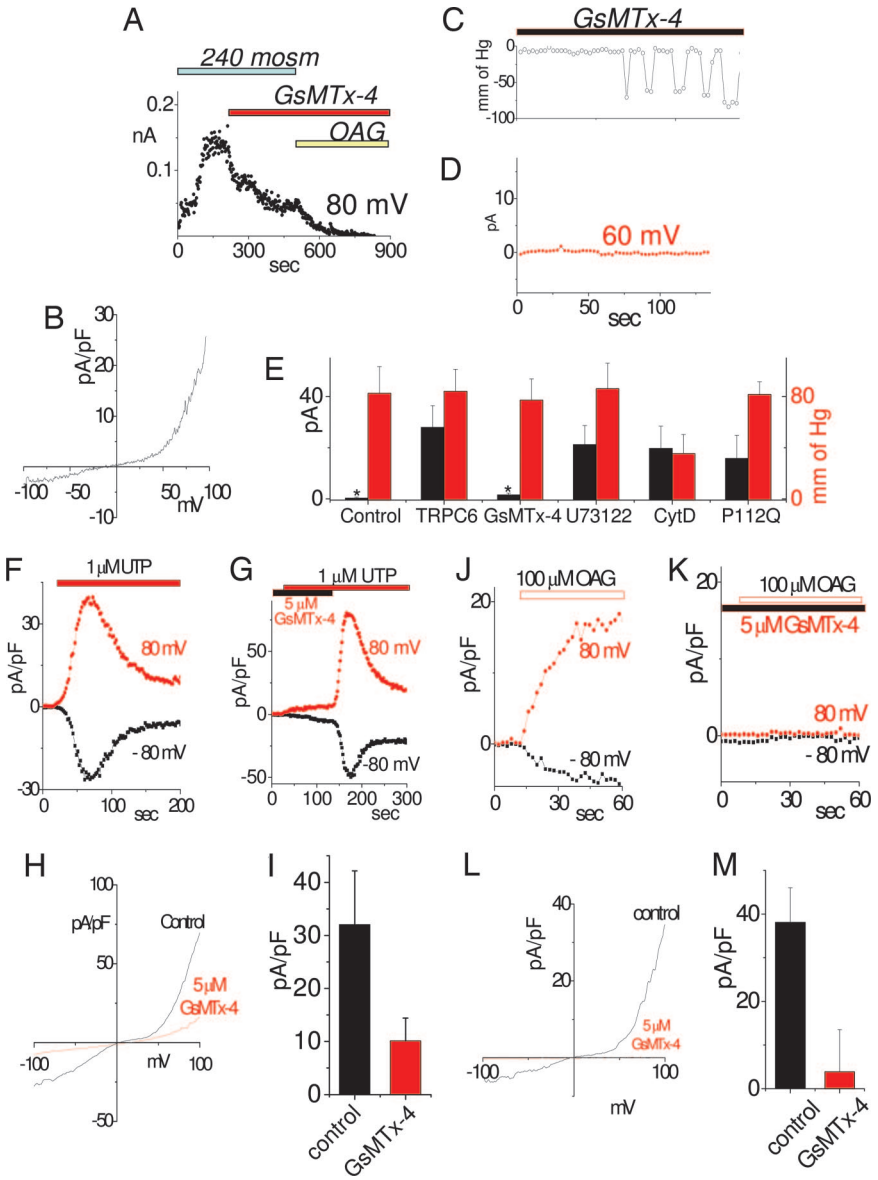

Fig. 3. Activation of TRPC6 channels in response to stretch, phospholipase C, or direct application of diacylglycerol, is inhibited by the tarantula peptide, GsMTx-4. (*A* and *B*) Inhibition of the hypoosmotic response of TRPC6 by GsMTx-4. (*A*) Acute addition of 5 μM GsMTx-4 to the activated TRPC6 increases the rate of channel inactivation. Currents are shown at 80 mV. (*B*) I/V relationship of the currents in *A* at maximal activation. (*C* and *D*) Inhibition by GsMTx-4 of stretch-activated current in CHO cells overexpressing TRPC6. Pressure pulses applied to an inside-out patch (*C*) did not activate TRPC6 after 2-min exposure to 5 μM GsMTx-4 added to the pipette solution (*D*). (*E*) Summary of the stretch-activated currents in inside-out patches from CHO cells overexpressing TRPC6. The bar chart represents control CHO cells, TRPC6-overexpressing cells in the presence of 5 μM GsMTx-4, 20 μM U73122, 40 μM cytochalasin D, and TRPC6 P112Q-overexpressing cells. (*F–M*) Whole-cell recordings from CHO cells expressing TRPC6 in the absence or presence of 5 μM GsMTx-4 applied 20–40 min before the trace. Time course of TRPC6 activation by the purinergic receptor agonist UTP at −80 (black) and +80 (red) mV (*F*); UTP-induced TRPC6 activation was inhibited by GsMTx-4, and inhibition was reversed by washout (*G*); I/V relationship for maximal activation of TRPC6 channels in absence (black) and presence (red) of 5 μM GsMTx4 (*H*); average peak current at 100 mV in the absence (black) and presence (red) of GsMTx-4 (both cases, $n = 3$) (*I*); time-course of TRPC6 activation by 100 μM OAG (*J*); activation of TRPC6 by OAG is inhibited after incubation with 5 μM GsMTx-4 (*K*); examples of I/V relationship of maximal OAG-induced TRPC6 channel activation in the absence (black) and presence (red) of 5 μM GsMTx-4 (*L*); and average peak current at 100 mV in the absence (black) and presence (red,) of GsMTx-4 ($n = 3$ and 4, respectively) (*M*).

stretch. Overall, whereas TRPC6 may be a mechanosensor in podocytes, the mutational defect leading to podocyte malfunction is likely to alter a downstream effect in the transduction of mechanical sensing as opposed to the sensing process itself. Such downstream effects may be mediated by known physical interactions revealed by coimmunoprecipitation between TRPC6 and the cytoskeleton (25, 26).

Recent studies have revealed that the tarantula peptide, GsMTx-4, is a profound and specific inhibitor of stretch-activated channels (16, 27). The peptide blocks a range of stretch-activated channels but not by specific interactions with the channel proteins themselves because the synthesized enantiomer of GsMTx4 has the same effect (16). The peptide likely acts by inserting in the outer leaflet of the membrane and modifying the channel boundary lipids to favor the closed state (16). We therefore assessed the actions of GsMTx-4 on both the hypoosmotic- and pressure-induced activation of TRPC6 channels in HEK293 cells (Fig. 3). After activation of TRPC6 by treatment with hypoosmotic medium, application of

GsMTx-4 caused a rapid inhibition of the whole-cell current (Fig. 3*A*). We noted that application of OAG failed to activate any further current. In fact, it resulted in further inactivation. This is likely through activation of PKC, which is known to be inhibitory on the TRPC channels (4, 19). The I/V dependence at the maximal activation of the channel before application of the GsMTx-4 is shown in Fig. 3*B*. When pressure was applied to inside-out patches from CHO cells overexpressing TRPC6 and exposed for >2 min to 5 μM GsMTx-4, channel activation was blocked (Fig. 3 *C–D*). Repeated application of pressure pulses beyond the threshold of activation (Fig. 3*D*) resulted in no current in the presence of GsMTx-4. The GsMTx4 sensitivity is important, providing further evidence that the TRPC6 channel is a stretch sensor.

It is well known that members of the TRPC3/6/7 subfamily of channels are activated directly by the lipid DAG, either added exogenously to cells or generated in response to PLC-coupled receptors (4, 19, 28). We examined whether the receptor-induced activation of TRPC6 channels was modified by the GsMTx-4 peptide. As shown in Fig. 3*F*, the TRPC6 channel was activated in CHO cells in response to UTP-induced activation of P2Y receptors. Prior incubation with GsMTx-4 resulted in a substantial reduction in TRPC6 channel activation. This effect was reversible, thus, TRPC6 was fully activated by UTP after washout of the GsMTx-4 peptide (Fig. 3*G*). The I/V curve at maximal activation (Fig. 3*H*) reveals that the peptide-insensitive current has a more linear relationship, perhaps signifying that not all of the current is carried by TRPC6. The peptide reduced the maximal activation of TRPC6 by >65% (Fig. 3*I*). Application of the membrane-permeant DAG derivative OAG to TRPC6-expressing CHO cells also resulted in TRPC6 channel activation (Fig. 3*J*). Again, in the presence of GsMTx-4, this activation was reduced by ≈90% (Fig. 3 *K–M*). This is an important result, indicating that the action of the peptide on lipid-induced activation is analogous to its action in blocking stretch-activation of TRPC6 channels.

The results presented here reveal that TRPC6 channels can be activated not only in response to PLC-coupled receptors but also in response to mechanical stimuli. The latter effect is independent of PLC activation and likely occurs through sensing membrane lipid stretch. The blocking effect of GsMTx-4 on both responses indicates a fundamental link between these two activation mechanisms. The GsMTx-4 peptide isolated from tarantula venom is a specific modifier of nonselective mechanosensitive channels (27). Its inhibitory action is within the outer membrane leaflet and is considered to be through altering the distortion of the boundary lipids adjacent to the channel that occurs during membrane stretch (16, 17). Most likely, both activation processes produce an open channel through changes in lipid-channel interactions, and GsMTx4 disrupts these interactions by insertion in the membrane at the lipid-channel boundary. As shown in Fig. 4, we interpret the results to indicate that "mechanical sensing" of lipids may be fundamentally similar to "chemical sensing" of DAG by TRPC6. In this model, we compare the interaction between DAG (a lipid bearing a minimal head group) and the TRPC6 channel, with the effects of membrane stretch that are considered to exert a thinning of the lipid bilayer. Without addition of lipids to the bilayer, stretch necessarily causes bilayer thinning, and we hypothesize that membrane thinning exposes components of the TRPC6 protein that leads to channel activation (Fig. 4 *A* and *B*). The action of the GsMTx-4 peptide is shown as inserting within the stressed lipid boundary and preventing channel activation (Fig. 4*C*). When TRPC6 channels are activated in response to PLC-coupled receptors, there is a rapid breakdown of the charged, large-head group lipid PIP_2 to form the uncharged, small-head group lipid DAG (Fig. 4*D*). TRPC channels interact directly with PIP_2 through a conserved lipid-binding domain (29), hence PLC-induced PIP_2 breakdown and DAG production may occur predominantly in the inner bilayer leaflet close to the channel. The small-head group DAG molecule would result in increased membrane stress depicted in Fig. 4*E* as a deflection of the inner leaflet and increased curvature known to be a major determinant of stretch-activated channels (30–33). This local curvature would cause increased stretch in the outer bilayer leaflet that would be akin to the effect of physical stretch applied to the whole bilayer. Again, the action of the GsMTx-4 peptide is shown as inserting within the stressed lipid boundary and preventing channel activation (Fig. 4*C*). Although OAG is added from the outside, it is highly membrane permeant and clearly activates TRPC6 analogously to DAG formed from PIP_2 breakdown in the inner leaflet (19). Hence, OAG likely associates with the channel in the inner leaflet. Overall, we consider that the effect of the GsMTx-4 peptide is to relieve lipid-mediated stress caused by either mechanical stretch or DAG production by altering the boundary lipid–protein interactions. GsMTx-4 peptide may stabilize the membrane by inserting at the lipid–channel boundary and preventing channel exposure.

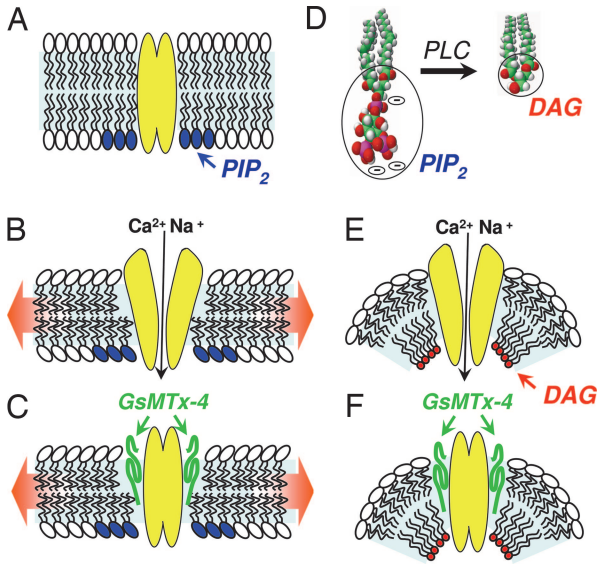

Fig. 4. Model of TRPC6 activation by stretch and diacylglycerol and the inhibition of this activation by the tarantula peptide, GsMTx-4. (*A*) The resting closed state of the channel is depicted with PIP_2 (blue head groups) in the inner leaflet vicinity of the channel. (*B*) Stretch of the cell membrane causes membrane thinning, inducing exposure and/or conformational change in the TRPC6 channel, resulting in its open state. (*C*) The GsMTx-4 peptide inserts in the outer membrane leaflet and, by modifying boundary lipids, relieves lipid stress and/or prevents channel exposure resulting in channel closure. (*D*) Receptor activation of phospholipase C results in cleavage of the large charged IP_3 head group of PIP_2 to produce the small uncharged head group on DAG. (*E*) The drastic change in lipid geometry on the inner leaflet in the vicinity of the channel creates membrane curvature, resulting in stress and/or exposure of the TRPC6 channel and its opening. (*F*) As with stretch-activation, the GsMTx-4 peptide inserts in the outer bilayer leaflet and, by modifying channel boundary lipids, relieves lipid stress and/or prevents channel exposure and inhibits channel gating.

That TRPC6 channels are mechanosensitive has profound implications. Hemodynamic forces, shear stress, and stretch-induced Ca^{2+} signals are a major determinant of vascular cell morphology and function (12, 34). However the gating mechanisms and the mechanical sensors that mediate the response to hemodynamic force have not been clarified. The presence and function of TRPC channels in smooth muscle is well known (5, 6, 35). Smooth muscle cells display an array of TRPC channels, with a preponderance of TRPC1 and TRC6 (5, 6, 35). Recent studies have revealed that TRPC6 channels in vascular smooth muscle regulate myogenic tone in response to intravascular pressure in small arteries (9). It was assumed that the TRPC6 channel was activated indirectly as a result of PLC-coupled stretch receptors (9). Our results reveal that TRPC6 channels are likely the direct sensors of mechanical stretch

as well as DAG. Excessive smooth muscle proliferation in patients with idiopathic pulmonary arterial hypertension (IPAH) has been linked to elevated expression of TRPC6 (15), hence the disease may be mediated by increased mechanical sensitivity with higher TRPC6 expression. Recently, TRPC6$^{-/-}$ mice were revealed to have elevated blood pressure, which was linked to a compensatory overexpression of TRPC3 channels. Based on the close sequence similarity of TRPC3 and TRPC6 channels, TRPC3 may have similar mechanosensitive properties and, hence, their high expression may overcompensate for TRPC6 loss and result in increased pressure-induced blood vessel constriction and, hence, elevated blood pressure. Overall, the functioning of TRPC6 channels as mechanosensors correlates well with TRPC6 expression pattern in tissues that are subject to hydrostatic forces. TRPC6 is highly expressed in vascular smooth muscle (7) and the myogenic tone response is mediated by depolarization leading to activation of L-type Ca^{2+} channels (10, 11). As a mechanosensor and nonselective cation channel, TRPC6 is therefore a prime candidate for the role of mechanical transducer in smooth muscle.

Materials and Methods

Cell Culture and Reagents. HEK-293 and CHO cells were grown in DMEM and F-12K medium, respectively, with 10% FBS and 1% P/S. GsMTx-4 peptide was from Peptides International (Louisville, KY) and was freshly dissolved before use. UTP and OAG were from Sigma (St. Louis, MO). Enhanced YFP vector and TRPC6 vector were from BD Biosciences (Mountain View, CA).

DNA Expression Constructs and Mutagenesis. The TRPC6 (GenBank accession no. Q9Y210) was subcloned into psDNA3 (Stratagene, La Jolla, CA). The TRPC6 P112Q mutation was introduced by using the QuikChange site-directed mutagenesis kit (Stratagene) and confirmed by sequencing. Cells were cotransfected with YFP plus vectors described, and YFP-expressing cells were selected by fluorescence (19). Transfections were performed by electroporation by using the Gene Pulser II electroporation system (Bio-Rad, Hercules, CA) at 350 V, 960 μF, and infinite resistance.

Electrophysiology. Cells were incubated on poly-L-lysine-coated coverslips after transfection for 24–48 h and transferred into the recording chamber before the experiment. Immediately after establishment of the whole-cell/inside-out configuration, voltage ramps of 50-ms duration spanning the voltage range of −100 to +100 mV, followed by a 350-ms step to −60 mV and +60 mV were delivered continuously. Currents were filtered at 6 kHz and sampled at 50-μs intervals. Some of the currents were filtered off-line at 1–3 kHz for presentation purposes. We used automatic capacitive and series resistance compensation of the EPC-10 amplifier (HEKA, Southboro, MA). PatchMaster, Pulsetools, FitMaster, Excel, and Origin software were used for acquisition and analysis. The temporal development of inward (at −80 mV) and outward (+80 mV) currents from whole-cell recordings were measured from the individual ramps at each time point. The time courses of the currents from inside-out patches were derived from an average of the 200-ms currents at ±60 mV at each time point and corrected for seal changes. GsMTx-4 was added to the external solution 20–40 min. before experiments for whole-cell recordings and in the pipette for inside-out patches. Stretch responses in inside-out patches were tested ≈5 min after seal formation. The intracellular solution contained 145 mM CsGlu, 10 mM Hepes, 10 mM EGTA, 8 mM Na, 1 mM Mg, 2 mM Na-ATP, and 100 nM Ca-free (pH 7.2). ATP was omitted in some of the experiments. For extracellular solutions, we used 145 mM CsGlu, 2 mM MgCl2, 10 mM glucose, and 10 mM Hepes (pH 7.4). Osmolarity was manipulated by dilution of the solution, keeping the divalent ions concentration constant. We used a salt bridge for grounding glutamate-based external solutions. The I/V curves were derived from the current ramp at the time of maximum activation defined from the current-time dependence. All I/V curves are shown at the time of maximal activation. The currents before channel activation (average of three to five traces) were used for leak subtraction. The maximal TRPC6 currents at 100 mV were used for statistical analysis. Each statistical bar plot (Figs. 1*E* and 3 *E*, *I*, and *M*) is an average of three or more experiments.

Capacitance Measurements. Capacitance measurements were made in "sine + DC" mode of the EPC-10 software lock-in amplifier, with 1.25-kHz sinusoidal command voltage (40 mV peak to peak) that was superimposed on the holding potential of 0 mV. ΔCm were elicited by exposure to hypoosmotic solution in control cells, where channel gating was minimal.

We thank Thomas Hofmann (Institut für Pharmakologie und Toxikologie, Marburg, Germany) for kindly providing us with the HEK-TRPC6-inducible cell line, Frederick Sacks and Alexander Petrov for critical reading of the manuscript, and Martin Schneider and X. D. Tang for helpful discussions. This work was supported by National Institutes of Health Grants HL 55426 and AI 58173.

1. Ramsey IS, Delling M, Clapham DE (2006) *Annu Rev Physiol* 68:619–647.
2. Montell C (2005) *Sci STKE* 2005, re3.
3. Putney JW (2005) *Pflugers Arch* 451:29–34.
4. Venkatachalam K, van Rossum DB, Patterson RL, Ma HT, Gill DL (2002) *Nat Cell Biol* 4:E263–E272.
5. Xu SZ, Beech DJ (2001) *Circ Res* 88:84–87.
6. Beech DJ, Muraki K, Flemming R (2004) *J Physiol* 559:685–706.
7. Soboloff J, Spassova MA, Xu W, He LP, Cuesta N, Gill DL (2005) *J Biol Chem* 280:39786–39794.
8. Dietrich A, Kalwa H, Rost BR, Gudermann T (2005) *Pflugers Arch* 451:72–80.
9. Welsh DG, Morielli AD, Nelson MT, Brayden JE (2002) *Circ Res* 90:248–250.
10. Davis MJ, Hill MA (1999) *Physiol Rev* 79:387–423.
11. Welsh DG, Nelson MT, Eckman DM, Brayden JE (2000) *J Physiol* 527 (Pt 1):139–148.
12. Standley PR, Obards TJ, Martina CL (1999) *Am J Physiol* 276:E697–E705.
13. Reiser J, Polu KR, Moller CC, Kenlan P, Altintas MM, Wei C, Faul C, Herbert S, Villegas I, Avila-Casado C, *et al.* (2005) *Nat Genet* 37:739–744.
14. Maroto R, Raso A, Wood TG, Kurosky A, Martinac B, Hamill OP (2005) *Nat Cell Biol* 7:179–185.
15. Yu Y, Fantozzi I, Remillard CV, Landsberg JW, Kunichika N, Platoshyn O, Tigno DD, Thistlethwaite PA, Rubin LJ, Yuan JX (2004) *Proc Natl Acad Sci USA* 101:13861–13866.
16. Suchyna TM, Tape SE, Koeppe RE, Andersen OS, Sachs F, Gottlieb PA (2004) *Nature* 430:235–240.
17. Suchyna TM, Johnson JH, Hamer K, Leykam JF, Gage DA, Clemo HF, Baumgarten CM, Sachs F (2000) *J Gen Physiol* 115:583–598.
18. Hofmann T, Obukhov AG, Schaefer M, Harteneck C, Gudermann T, Schultz G (1999) *Nature* 397:259–263.
19. Venkatachalam K, Zheng F, Gill DL (2003) *J Biol Chem* 278:29031–29040.
20. Dietrich A, Schnitzler M, Emmel J, Kalwa H, Hofmann T, Gudermann T (2003) *J Biol Chem* 278:47842–47852.
21. Shi J, Mori E, Mori Y, Mori M, Li J, Ito Y, Inoue R (2004) *J Physiol* 561:415–432.
22. Honore E, Patel AJ, Chemin J, Suchyna T, Sachs F (2006) *Proc Natl Acad Sci USA* 103:6859–6864.
23. Gottlieb PA, Suchyna TM, Ostrow LW, Sachs F (2004) *Curr Drug Targets CNS Neurol Disord* 3:287–295.
24. Winn MP, Conlon PJ, Lynn KL, Farrington MK, Creazzo T, Hawkins AF, Daskalakis N, Kwan SY, Ebersviller S, Burchette JL, *et al.* (2005) *Science* 308:1801–1804.
25. Gudermann T (2005) *Nat Genet* 37:663–664.
26. Goel M, Sinkins W, Keightley A, Kinter M, Schilling WP (2005) *Pflugers Arch* 451:87–98.
27. Ostrow KL, Mammoser A, Suchyna T, Sachs F, Oswald R, Kubo S, Chino N, Gottlieb PA (2003) *Toxicon* 42:263–274.
28. Montell C (1998) *Curr Opin Neurobiol* 8:397.
29. van Rossum DB, Patterson RL, Sharma S, Barrow RK, Kornberg M, Gill DL, Snyder SH (2005) *Nature* 434:99–104.
30. Riske KA, Dobereiner HG (2003) *Biophys J* 85:2351–2362.
31. Markin VS, Sachs F (2004) *Phys Biol* 1:110–124.
32. Nielsen C, Andersen OS (2000) *Biophys J* 79:2583–2604.
33. Petrov AG, Usherwood PN (1994) *Eur Biophys J* 23:1–19.
34. Riha GM, Lin PH, Lumsden AB, Yao Q, Chen C (2005) *Ann Biomed Eng* 33:772–779.
35. Jung S, Strotmann R, Schultz G, Plant TD (2002) *Am J Physiol* 282:C347–C359.